PHYSICAL REVIEW B VOLUME 34, NUMBER 12 15 DECEMBER 1986

Dynamics of photoexcited carriers sinking into an enlarged well in a GaAs/AlAs short-period superlattice

A. Nakamura
Department of Applied Physics, Faculty of Engineering, Nagoya University, Chikusa-ku, Nagoya 464, Japan

K. Fujiwara, Y. Tokuda, and T. Nakayama
Central Research Laboratory, Mitsubishi Electric Corporation, Amagasaki, Hyogo 661, Japan

M. Hirai
Department of Applied Physics, Faculty of Engineering, Tohoku University, Sendai 980, Japan

(Received 8 September 1986)

We report on the dynamics of photoexcited carriers using picosecond luminescence measurements of GaAs/AlAs superlattices with a barrier width of 1.2 nm and a well width of 3.4 nm. The observed decay kinetics allow us to observe the tunneling-assisted radiative recombination of electrons and holes in different wells. Furthermore, introducing an enlarged well in the superlattice, we investigate the dynamics of photoexcited carriers sinking into the deeper well via vertical transport.

Dynamics of photoexcited carriers in a semiconductor superlattice has recently received considerable interest. Much attention has been paid to the carrier dynamics within the well because of the two-dimensional properties.[1-4] If the width of the barrier is reduced up to the order of 1 nm, the tunneling of carriers through the barrier occurs dominantly and sublevels in the wells form minibands.[5] In such a superlattice with thin barriers, i.e., short-period superlattice (SPS), we can expect a vertical transport of photoexcited carriers and "a tunneling-assisted radiative recombination" between electrons and holes in different wells. Very recently, Deveaud *et al.*[6] reported the vertical transport observed by the picosecond spectroscopy at 5 K. However, they could not observe this recombination with tunneling, since excitons are formed at low temperature. In addition, the decay kinetics of excitons becomes more complicated at low temperature because of the phonon-assisted cross relaxation between localized exciton states as was shown by Masumoto, Shionoya, and Kawaguchi.[3] Therefore, a study of time behavior of emission due to the electron-hole recombination is necessary to investigate the carrier dynamics across the heterostructures.

In this Rapid Communication, we report on dynamics of photoexcited carriers which sink into an enlarged single quantum well (SQW) introduced in GaAs/AlAS SPS structures with a well width of 3.4 nm and a barrier width of 1.2 nm. A carrier transport across the heterostructures in the SPS at 77 K was investigated by measuring picosecond time behavior of luminescence from the two kinds of SPS samples with or without an enlarged SQW. The carrier lifetimes of the SPS layers in the sample with SQW decrease compared to that of the sample without SQW. Furthermore, time evolution of SQW emission is delayed and the intensity increase corresponds to the decrease in the SPS emission. This time behavior directly reflects the vertical transport of photoexcited carriers across the heterostructures. From the quantitative analysis of decay curves on the basis of rate equations of photoexcited carriers in SPS layers and SQW, we could elucidate dynamics of carriers sinking into SQW via vertical transport. This also allowed us to find the radiative recombination process with tunneling through the barriers in the SPS structure.

The GaAs/AlAs SPS structures studied here were grown by molecular beam epitaxy (MBE) on (100) GaAs substrates.[7] The growth sequence for the SPS sample without SQW (we named it No. 3) consisted of 0.2 μm of GaAs buffer, 1.4 μm of $Al_{0.4}Ga_{0.6}As$ lower cladding, 80 periods of the GaAs/AlAs SPS, and 0.2 μm of $Al_{0.4}Ga_{0.6}As$ cap layers. In the SPS sample with SQW (No. 2), 6.1 nm of GaAs was introduced above the 40 periods of the GaAs/AlAs SPS and confined by 40 periods of the same SPS. Thus, the two types of samples differ only by the introduction of the SQW. To examine influences of unknown growth conditions on carrier dynamics, we made another sample (No. 1) in which 10 periods of $GaAs/Al_{0.4}Ga_{0.6}As$ multiple quantum well (MQW) buffer ($L_z = L_B = 10$ nm) were grown between the GaAs buffer and the $Al_{0.4}Ga_{0.6}As$ lower cladding keeping the same SPS and SQW structures.

The experiment was performed by using a synchronously mode-locked dye laser with 613.4 nm of wavelength and about 10 ps of pulse width. The excitation intensity was ~ 150 mW/cm^2. Time evolution of emission intensity was measured by a time-correlated single-photon counting method. The time resolution of about 50 ps was obtained for decay curves using a convolutional analysis. The emission from the three samples was collected in the backward direction with the same configuration in order to compare relative intensities of these samples.

Figure 1 represents emission spectra of three samples (No. 1, No. 2, and No. 3) at 77 K with excitation of a cw dye laser ($\lambda = 613.4$ nm). In the SPS without SQW (No. 3), two emission bands are observed and assigned to the emission due to the $n = 1$ electron-light-hole (lh) transition (E_{1lh}^{SPS}) and $n = 1$ electron-heavy-hole (hh) transition (E_{1hh}^{SPS}) from the higher-energy side. In the SPS with the

© 1986 The American Physical Society

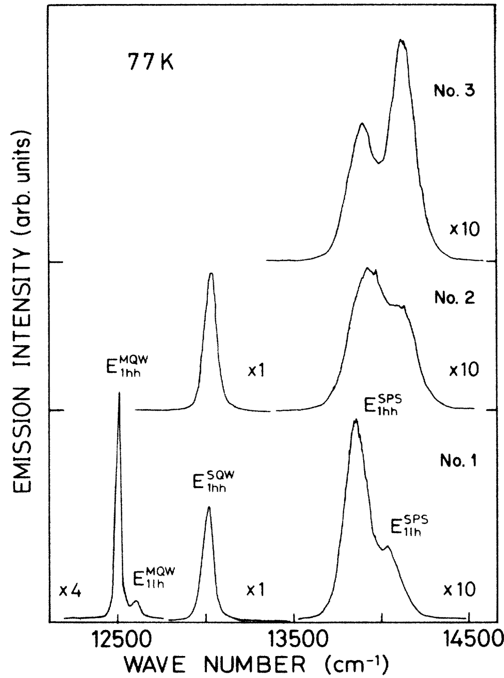

FIG. 1. Emission spectra of the samples No. 1–3 at 77 K. E_{1hh}^{SPS} and E_{1lh}^{SPS} are due to $n=1$ electron–heavy-hole transition and $n=1$ electron–light-hole transition of the SPS layers, respectively, and E_{1hh}^{MQW} and E_{1lh}^{MQW} are those of the MQW. E_{1hh}^{SQW} is due to $n=1$ electron–heavy-hole transition of the SQW.

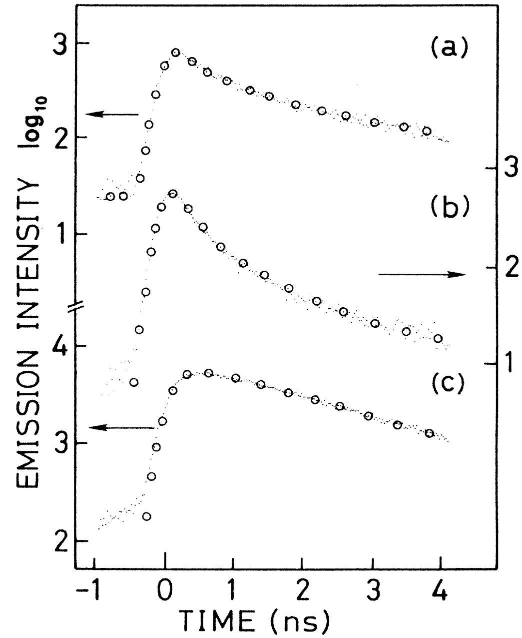

FIG. 2. Decay curves measured at the peak positions of E_{1hh}^{SPS} and E_{1hh}^{MQW} bands. (a) E_{1hh}^{SPS} band of the sample No.3, (b) E_{1hh}^{SPS} band of No. 2, and (c) E_{1hh}^{SQW} band of No. 2. Open circles represent calculated curves by the convolution of solutions of rate equations with the instrumental response.

SQW (No. 2), the emission band associated with $n=1$ electron–heavy-hole transition of the SQW (E_{1hh}^{SQW}) is observed in addition to the emission from the SPS layers. In the sample No. 1, two emission bands which originate from the MQW are also observed (E_{1lh}^{MQW} and E_{1hh}^{MQW}). The intensity of luminescence from the SPS layers of the samples No. 2 and No. 1 decreases compared to that of the SPS layers without SQW (No. 3). The intensity of the SQW emission is quite strong in spite of the small volume. This suggests that photoexcited carriers in the SPS layers diffuse across the heterostructures to be trapped effectively to the enlarged well.

To investigate carrier dynamics by the vertical transport, we have performed measurements of time evolution of emission intensity in the picosecond time region. In Fig. 2 are shown decay curves of the E_{1hh}^{SPS} emission bands and the E_{1hh}^{SQW} emission band. In curves (a) and (b), the time behavior does not exhibit single exponential decay and seems to be decomposed into fast and slow components. As displayed in curve (b) of Fig. 2, the introduction of the enlarged well in the SPS structure causes the decrease in the carrier lifetimes. The emission bands due to $n=1$ electron–light-hole transition exhibit completely the same time behavior as the E_{1hh}^{SPS} bands. This implies that light- and heavy-hole bands are strongly mixed and holes in these bands are thermally in equilibrium at 77 K. In curve (c) of Fig. 2, the time behavior of the SQW emission is shown. We should note the delayed rise corresponding to the decrease in the SPS emission.

In what follows, we will quantitatively analyze the experimental results on the basis of a rate equation model for photoexcited carriers in both the SPS layers and the SQW. We consider only kinetics of electron population, since the excitation density is low (150 mW/cm^2) and undoped GaAs contains residual acceptors with $N_A - N_D = 10^{14} \sim 10^{15}\ cm^{-3}$. The GaAs quantum wells in the SPS structures are uniformly excited by the exciting laser (613.4 nm) because of the small well thickness. Since the barrier width of the samples studied here is 1.2 nm, the tunneling of carriers through the barrier effectively takes place. Thus, we can expect the tunneling-assisted recombination between electrons and holes which are bound in different wells as well as the direct recombination within the same well. In Fig. 3 we display schematically such processes for the electron-hole recombination. Holes in the lth well can recombine with the electrons in the mth or nth well as well as those in the lth well, since the electrons in the mth or nth well tunnel through the barrier to be found simultane-

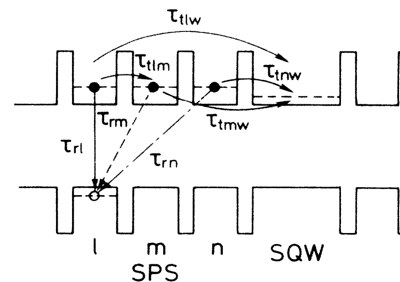

FIG. 3. Schematic diagram of processes of the direct recombination and the tunneling-assisted radiative recombination in the SPS structures with the enlarged well.

ously in the lth well. τ_{rl} is a radiative recombination time of electrons and holes in the same well and τ_{rm}, τ_{rn} are radiative lifetimes of the recombination between holes in the lth well and electrons in the nearest well (mth well) and those in the next-nearest well (nth well), respectively. Since the photon energy of the recombination via the tunneling between different wells is thought to be the same as that of the direct recombination in the same well, the observed emission from the SPS layers is the superposition of these processes. Therefore, we consider the following rate equations for electrons in the lth, mth, and nth wells taking into account the tunneling across the barriers. Assuming that the SPS layers are uniformly excited, rate equations for the carrier kinetics of the samples without SQW are

$$\frac{dN_l^0}{dt}=G(t)-\frac{N_l^0}{\tau_l^0},\ \frac{1}{\tau_l^0}=\frac{1}{\tau_{rl}}+\frac{1}{\tau_{tlm}}+\frac{1}{\tau_{\mathrm{nr}}}\ , \tag{1}$$

$$\frac{dN_m^0}{dt}=G(t)-\frac{N_m^0}{\tau_m^0},\ \frac{1}{\tau_m^0}=\frac{1}{\tau_{rm}}+\frac{1}{\tau_{\mathrm{nr}}}\ , \tag{2}$$

$$\frac{dN_n^0}{dt}=G(t)-\frac{N_n^0}{\tau_n^0},\ \frac{1}{\tau_n^0}=\frac{1}{\tau_{rn}}+\frac{1}{\tau_{\mathrm{nr}}}\ , \tag{3}$$

where N_l^0, N_m^0, and N_n^0 are electron densities in the lth, mth, and nth wells, respectively, and τ_{tlm} is the inverse of the tunneling rate, i.e., the transfer time between the lth well and the mth well. $G(t)$ is the generation of electrons and holes by exciting pulses. τ_{nr} is the nonradiative lifetime including all nonradiative processes. For the direct recombination process, we took into account the decay term due to the tunneling, since the tunneling is one of the decay channels for the electrons that recombine with holes in the same well.[8] For the tunneling-assisted recombination process, however, this term is not included in Eqs. (2) and (3), since this process is already considered by the periodic arrangement of quantum wells in the SPS.

Similarly, rate equations for the electron kinetics of the sample with the SQW are given as follows, considering the diffusion to the SQW:

$$\frac{dN_l^w}{dt}=G(t)-\frac{N_l^w}{\tau_l^w},\ \frac{1}{\tau_l^w}=\frac{1}{\tau_l^0}+\frac{1}{\tau_{tlw}}\ , \tag{4}$$

$$\frac{dN_m^w}{dt}=G(t)-\frac{N_m^w}{\tau_m^w},\ \frac{1}{\tau_m^w}=\frac{1}{\tau_m^0}+\frac{1}{\tau_{tmw}}\ , \tag{5}$$

$$\frac{dN_n^w}{dt}=G(t)-\frac{N_n^w}{\tau_n^w},\ \frac{1}{\tau_n^w}=\frac{1}{\tau_n^0}+\frac{1}{\tau_{tnw}}\ , \tag{6}$$

$$\frac{dN_{\mathrm{SQW}}}{dt}=g(t)+\frac{N_l^w}{\tau_{tlw}}+\frac{N_m^w}{\tau_{tmw}}+\frac{N_n^w}{\tau_{tnw}}-\frac{N_{\mathrm{SQW}}}{\tau_{\mathrm{SQW}}}\ ,\quad \frac{1}{\tau_{\mathrm{SQW}}}=\frac{1}{\tau_{r\mathrm{SQW}}}+\frac{1}{\tau_{\mathrm{nr}\,\mathrm{SQW}}}\ , \tag{7}$$

where τ_{tlw}, τ_{tmw}, and τ_{tnw} are the times of tunneling transfer to the SQW which have approximately the same value and can be replaced by an effective transfer time τ_{tw}. $\tau_{r\mathrm{SQW}}$ and $\tau_{\mathrm{nr}\mathrm{SQW}}$ are the radiative and non-radiative lifetimes of SQW, respectively.

The time evolution of emission intensity for each process is written as

$$I_i^j(t)=\frac{1}{\tau_{ri}}N_i^j(t),\ i=l,m,n,\text{ and } j=0,w\ . \tag{8}$$

Therefore, the decay curves of emission from the SPS layers are the sum of the three exponential functions with different time constants, τ_i^j ($i=1$, m, n, and $j=0,w$). Numerical solutions of Eqs. (1)–(3) for the sample without the SQW are fitted to the observed decay curve as adjustable parameters of decay times and the relative amount of the three components. The best fitted curve is shown by open circles in curve (a) of Fig. 2. The values of decay times are summarized in Table I. The decay time for the direct recombination of electrons and holes in the same well is 0.3 ns. The decay time for the recombination of holes with electrons in the nearest well via the tunneling is 1.9 ns and that for the recombination of holes with electrons in the next nearest well is ~ 10 ns. Since the period of the exciting pulse train in our measuring system is 12 ns, we could not measure decay curves at delay times longer than ~ 5 ns. As a result, the long decay time was not accurately determined. Nevertheless, if we do not consider the third component with slow decay, we could not obtain the best fit between the experimental and calculated curves at both the initial stage and the late stage. Consequently, the above analysis based on the rate equations allowed us to find the tunneling-assisted recombination of electrons and holes in the different wells. This can be compared to the tunneling-assisted emission in compensated GaAs with heavy doping[9] and the photon-assisted tunneling across a GaAs p-n junction with forward bias.[10] In addition to the radiative recombination process, we note that the nonradiative process such as the interface recombination in the heterostructure may be included to shorten the measured decay times.

Similarly, we have calculated a decay curve for the SPS luminescence of the sample with the SQW. From the best fit of the calculated curve, we have found the decrease in the decay times for each component. This decrease results from the sinking of photoexcited carriers in the SPS into the SQW. These values are also summarized in Table I. By using the values of τ_l^0, τ_m^0, τ_n^0, τ_l^w, τ_m^w, τ_n^w, we can determine the time of the electron sinking into the SQW; $\tau_{tlw}=0.6$ ns, $\tau_{tmw}=1.1$ ns, and $\tau_{tnw}\sim 4.5$ ns. These times should give approximately the same value, which is an averaged or effective time of sinking. The value of τ_{tlw} is very sensitive to the experimental errors for the determination of the decay times, since they are short. Considering the experimental accuracy of our measuring method, which is about 50 ps, τ_{tlw} is in the range of $0.4\sim 1.2$ ns.

TABLE I. The values of decay times, τ_i^j ($i=l$, m, n, and $j=0$, w), τ_{SQW}, and a rise time τ_R for $E_{1\mathrm{hh}}^{\mathrm{SPS}}$ and $E_{1\mathrm{hh}}^{\mathrm{SQW}}$ bands of the samples No. 1–3. All decay times are in units of ns.

	τ_l^0,τ_l^w	τ_m^0,τ_m^w	τ_n^0,τ_n^w	τ_{SQW}	τ_R
No. 3	0.3	1.9	~ 10	···	···
No. 2	0.2	0.7	3.1	1.9	0.2
No. 1	0.2	0.7	3.1	1.6	0.2

Thus, $\tau_{tlw} \simeq \tau_{tmw}$. However, τ_{tnw} is larger than this value. This discrepancy might arise from the poor accuracy for the slow decay component. Consequently, we have found that the time during which photoexcited carriers sink into the enlarged well by the vertical transport is about 1 ns in the SPS structures studied here.

Decay kinetics of the SQW emission will be analyzed from Eq. (7). The solution of this equation gives two components; a fast-rise component which originates from the directly excited carriers in the SQW by the exciting pulse, and a delayed component with a rise time due to the vertical transport from the SPS layers. We could obtain the best fit by choosing the effective rise time τ_R of 0.2 ns and the decay time of 1.9 ns. The intensity ratio of the component due to the vertical transport to the direct excitation component is 3.3. Therefore, most of the photoexcited carriers in the SQW which contribute to the luminescence arise from the carriers that are excited in the SPS layers. This is consistent with the strong luminescence of the SQW in spite of the small volume.

Next, we will give further evidence for the validity of our analysis based on the rate equations from the relation of the time-integrated intensity and the lifetimes. From Eqs. (1), (2), (4), (5), and (8) we can get the following relations for the time-integrated intensities of each component:

$$I_i^j = N_0 \frac{\tau_i^j}{\tau_{ri}}, \; i = l, m, \text{and } j = 0, w \quad (9)$$

where N_0 is the electron density at $t=0$. Thus, the intensity ratios I_l^w/I_l^0 and I_m^w/I_m^0 are equal to the ratios τ_l^w/τ_l^0 and τ_m^w/τ_m^0, respectively. Using the values shown in Table I, we obtain $\tau_l^w/\tau_l^0 = 0.67$, $\tau_m^w/\tau_m^0 = 0.37$ for both sets of the samples (No.2 + No. 3 and No. 1 + No. 3). On the other hand, the time-integrated intensities of each component can be calculated from the decay curves of the SPS emission. We estimated the sum of the time-integrated intensities of the decay curves which were measured at the peak positions of the $E_{1\text{hh}}^{\text{SPS}}$ and $E_{1\text{lh}}^{\text{SPS}}$ bands. This intensity is proportional to the total emission intensities of SPS layers, since the linewidth of these bands is similar and it is unchanged by the introduction of the SQW. The ratios obtained by this procedure are $I_l^w/I_l^0 = 0.53$ and $I_m^w/I_m^0 = 0.21$ for No. 2 + No. 3 and $I_l^w/I_l^0 = 0.65$ and $I_m^w/I_m^0 = 0.40$ for No. 1 + No. 3. Comparing them with the ratios, τ_l^w/τ_l^0 and τ_m^w/τ_m^0, we find that the ratio calculated from the time-integrated intensities is in good agreement with that deduced from the decay times within the experimental accuracy of the relative intensities of the three samples. Therefore, this confirms that the values of decay times were unambiguously determined from the best fit between the experiments and calculations. We should also note that these ratios are independent of the samples studied. This demonstrates the reproducibility of the SPS heterostructures by our MBE system. As a result, we can conclude that the change in the time behavior by the introduction of the enlarged well in the SPS structures originates from the intrinsic properties and reflects the dynamics of the carriers sinking into the deeper well via the vertical transport in the SPS.

In summary, we have measured the time behavior of luminescence from the GaAs/AlAs SPS structures with the barrier width of 1.2 nm in the picosecond time region. The quantitative analysis of the decay kinetics allowed us to find that holes can recombine with electrons in the nearest and the next-nearest wells via the tunneling through the barriers. Furthermore, introducing an enlarged well in the SPS structures, we have demonstrated the dynamics of photoexcited carriers which sink into the deeper well via the vertical transport. The sinking time was determined to be about 1 ns in the SPS structures studied in the present work.

This work was supported in part by Scientific Research Grants-in-Aid No. 58540163 and No. 61540221 from the Ministry of Education, Science, and Culture of Japan.

[1]E. O. Gobel, H. Jung, J. Kuhl, and K. Ploog, Phys. Rev. Lett. **51**, 1588 (1983).

[2]J. F. Ryan, R. A. Taylor, A. J. Turberfield, A. Maciel, J. M. Worlock, A. C. Gossard, and W. Wiegmann, Phys. Rev. Lett. **53**, 1841 (1984).

[3]Y. Masumoto, S. Shionoya, and H. Kawaguchi, Phys. Rev. B **29**, 2324 (1984).

[4]J. E. Fouquet and A. E. Siegman, Appl. Phys. Lett. **46**, 280 (1985).

[5]R. Dingle, A. C. Gossard, and W. Wiegmann, Phys. Rev. Lett. **34**, 1327 (1975).

[6]B. Deveaud, A. Chomette, B. Lambert, A. Regreny, R. Romestain, and P. Edel, Solid State Commun. **57**, 885 (1986).

[7]K. Fujiwara, A. Nakamura, Y. Tokuda, T. Nakayama, and M. Hirai, Appl. Phys. Lett. (to be published).

[8]Y. Masumoto, S. Tarucha, and H. Okamoto, Phys. Rev. B **33**, 5961 (1986).

[9]J. Pankove, *Optical Processes in Semiconductors* (Prentice-Hall, Englewood Cliffs, 1971), p. 151.

[10]J. Pankove, Phys. Rev. Lett. **9**, 283 (1962).